

X-ray Filament with a Strong 6.7 keV Line in the Galactic Center Region

Shigeo YAMAUCHI¹, Miku SHIMIZU¹, Shinya NAKASHIMA², Masayoshi NOBUKAWA^{3, 4}, Takeshi Go TSURU³, and Katsuji KOYAMA^{3,5}

¹*Department of Physics, Nara Women's University, Kitauoyanishimachi, Nara 630-8506
yamauchi@cc.nara-wu.ac.jp*

²*Institute of Space and Astronautical Science/JAXA, 3-1-1 Yoshinodai, Chuo-ku, Sagami-hara, Kanagawa 252-5210*

³*Department of Physics, Graduate School of Science, Kyoto University,
Kitashirakawa-oiwake-cho, Sakyo-ku, Kyoto 606-8502*

⁴*The Hakubi Center for Advanced Research, Kyoto University, Yoshida-Ushinomiya-cho, Kyoto 606-8302, Japan*

⁵*Department of Earth and Space Science, Graduate School of Science, Osaka University,
1-1 Machikaneyama-cho, Toyonaka, Osaka 560-0043*

(Received ; accepted)

Abstract

An elongated X-ray source with a strong K-shell line from He-like iron (Fe XXVI) is found at (RA, Dec)_{J2000.0}=(17^h44^m00^s.0, -29°13'40''9) in the Galactic center region. The position coincides with the X-ray thread, G359.55+0.16, which is aligned with the radio non-thermal filament. The X-ray spectrum is well fitted with an absorbed thin thermal plasma (apec) model. The best-fit temperature, metal abundance, and column density are 4.1^{+2.7}_{-1.8} keV, 0.58^{+0.41}_{-0.32} solar, and 6.1^{+2.5}_{-1.3} × 10²² cm⁻², respectively. These values are similar to those of the largely extended Galactic center X-ray emission.

Key words: ISM: individual objects (Suzaku J174400–2913) — Galaxy: center — X-rays: ISM

1. Introduction

The central 300 pc of the Milky Way Galaxy (hereafter, the Galactic center: GC) is a unique region that contains many objects associated with high-energy phenomena. Due to its proximity, the GC would be one of the best region to investigate complex activity possibly originated from the central supermassive black hole.

Sagittarius (Sgr) A*, a bright compact radio source located at the dynamical center of the Galaxy, is a supermassive black hole of 4 × 10⁶ M_⊙ (e.g., Genzel et al. 2000; Ghez et al. 2000; Schödel et al. 2002; Eckart et al. 2002). Other than Sgr A*, the most striking structure is the "radio arc", consisting of a straight filament (called the spur) perpendicular to the Galactic plane and arched filament (called the bridge) along the Galactic plane (e.g., Genzel & Townes 1987; Genzel et al. 1994, and references therein). Previous radio observations revealed that the bridge is thermal while the spur is non-thermal origins. In addition, a number of non-thermal radio filaments (NTFs) that run roughly aligned perpendicular to the Galactic plane have been found (e.g., Yusef-Zadeh et al. 1984). The NTFs are due to synchrotron radiation from relativistic particles on local magnetic field.

Sgr A* is not X-ray bright; its luminosity is only ∼10³³ erg s⁻¹ (e.g., Baganoff et al. 2003) with sporadic small flares up to ∼10³⁵ erg s⁻¹ (e.g., Baganoff et al. 2001). However the discovery of time variable 6.4 keV (K-shell emission from Fe I) clouds indicates that Sgr A* had been more active of about ∼10^{39–40} erg s⁻¹, till about 50 years ago (e.g., Koyama et al. 1996; Ponti et al. 2010; Ryu et

al. 2013).

At present, the most prominent X-ray object in the GC region is a thin hot plasma with a temperature of ∼7 keV, the so-called Galactic Center X-ray Emission (GCXE) (Koyama et al. 1989, 1996, 2007c, Yamauchi et al. 1990). The total thermal energy of this plasma is huge, (∼10^{53–54} erg, Yamauchi et al. 1990; Koyama et al. 1996), and the plasma temperature is too high to confine in the GC against the Galactic gravity. Thus, its origin is still puzzling. In addition to the GCXE, some filamentary X-ray structures were discovered with Chandra and XMM-Newton in the GC region (Wang et al. 2002; Sakano et al. 2003; Lu et al. 2003, 2008; Johnson et al. 2009). Most of them exhibit featureless spectra with no sign of emission lines from highly ionized atoms, and hence they are likely to be in non-thermal nature.

G359.55+0.16 is one of the X-ray filament discovered with Chandra, and is named "X-ray thread" (Wang et al. 2002; Lu et al. 2003; Johnson et al. 2009). This source would have a cylindrical shape of 10'' diameter and 1–2' length, aligned with the NTF G359.54+0.18 (Lu et al. 2003; Yusef-Zadeh et al. 1997). Lu et al. (2003) concluded that G359.55+0.16 is likely to be a non-thermal emission. In fact, Johnson et al. (2009) reported that the X-ray spectrum is well represented by a power-law model with a photon index of 1.2^{+1.3}_{-1.1} and absorption with N_H=5.5^{+3.9}_{-3.6} × 10²² cm⁻². The energy flux in the 2–10 keV band was estimated to be 1.8 × 10⁻¹³ erg s⁻¹ cm⁻².

The Suzaku XIS has a better spectral resolution and lower/more stable intrinsic background than those of the

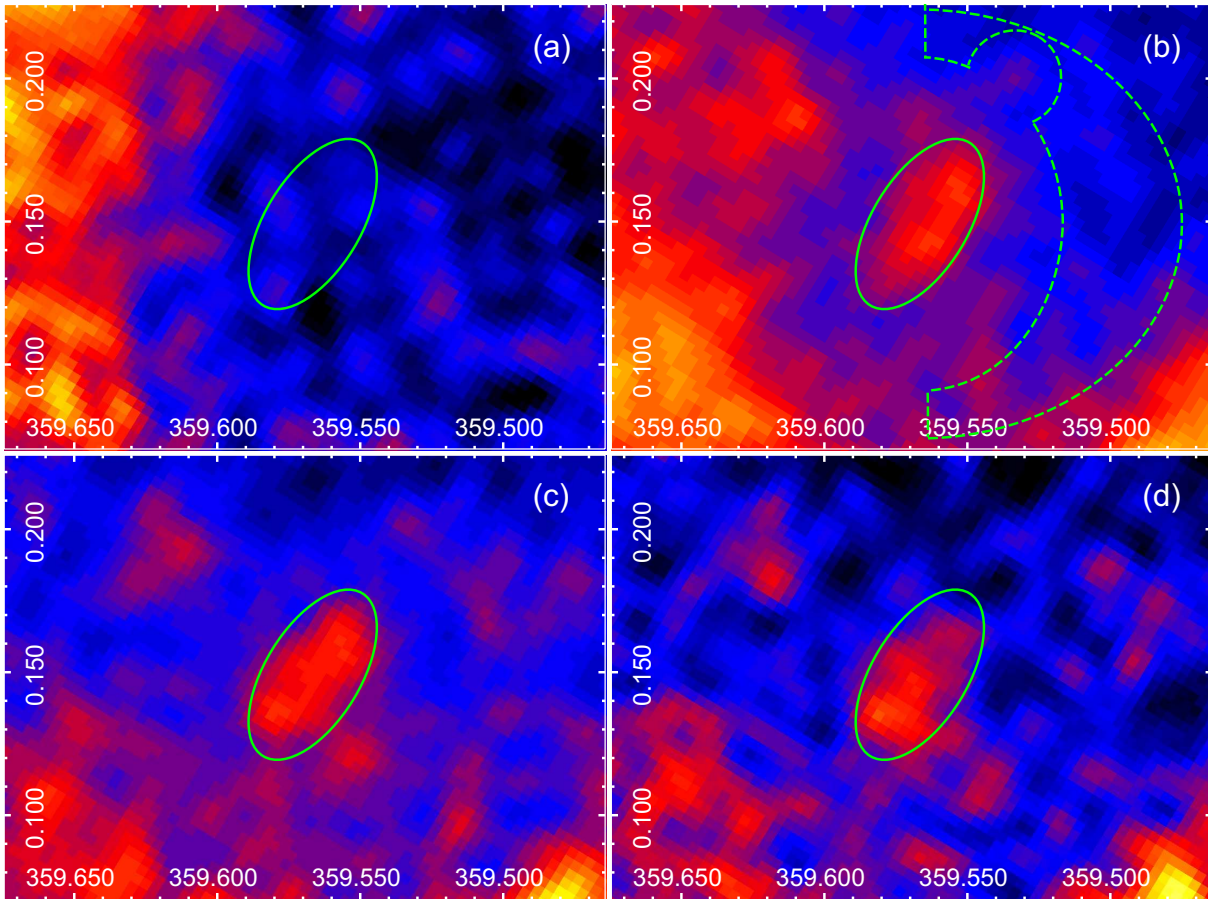


Fig. 1. XIS images in the (a) 1–2, (b) 2–5, and (c) 5–8, (d) 6.55–6.80 keV (Fe XXV- $K\alpha$). The coordinates are Galactic. All the available data acquired in the Galactic center region are utilized. Subtraction of the non-X-ray background and vignetting correction are performed. The green ellipses in all panels show a position of Suzaku J174400–2913 (a source region, see text), while the dashed line in (b) shows a background region.

previous X-ray satellites (Koyama et al. 2007a; Mitsuda et al. 2007), and hence it has the best sensitivity especially in the Fe K-shell line band. We carried out survey observations in the GC region with Suzaku and found an elongated emission with a strong Fe-K emission line (6.7 keV) at the position of G359.55+0.16. This paper reports the results of the spectral analysis of this elongated emission. Throughout this paper, the quoted errors are at the 90% confidence level.

2. Observation and Data Reduction

Survey observations in the GC region were carried out with the XIS (Koyama et al. 2007a) onboard Suzaku (Mitsuda et al. 2007). The XIS is composed of 4 CCD camera sensors placed at the focal planes of the thin foil X-ray Telescopes (XRT, Serlemitsos et al. 2007). XIS 1 is a back-side illuminated (BI) CCD, while XIS 0, 2, and 3 are front-side illuminated (FI) CCDs. The Field of view (FOV) of the XIS is $17'8 \times 17'8$. One of the FI sensors (XIS 2) became non-functional since 2006. Therefore, we used the data obtained with the other three sensors (XIS 0, 1, and 3). The XIS was operated in the normal clocking

mode with the time resolution of 8 s. The spectral resolution of the XIS was degraded due to the radiation of cosmic particles. In order to restore the XIS performance, the spaced-row charge injection (SCI) technique was applied. Details of the SCI technique are given in Nakajima et al. (2008) and Uchiyama et al. (2009).

The northwest of the GC field was observed on 2009 March 6 2:39:12 – March 9 2:55:25 (Obs. ID 503072010). The center position was $(\alpha, \delta)_{J2000.0} = (265^\circ 9883, -29^\circ 2111)$ [$(l, b) = (359^\circ 5753, +0^\circ 1669)$].

Data reduction and analysis were made with the HEASoft version 6.13. The XIS pulse-height data for each X-ray event were converted to Pulse Invariant (PI) channels using the `xispi` software and the calibration database version 2013-03-05. We rejected the data taken at the South Atlantic Anomaly, during the earth occultation, and at the low elevation angle from the earth rim of $< 5^\circ$ (night earth) and $< 20^\circ$ (day earth). After these screening, the exposure time was 140.6 ks.

3. Analysis and Results

3.1. Image

Figures 1a, 1b, 1c and 1d show the X-ray images in the 1–2, 2–5, 5–8, and 6.55–6.80 keV (Fe XXV- $K\alpha$) energy bands, respectively. The data of XIS 0, 1, and 3 were added to increase photon statistics. An elongated emission is found above 2 keV (figures 1b, 1c, and 1d), but no emission is seen below 2 keV (figure 1a). The center position of the elongated emission was determined to be (RA, Dec)_{J2000.0}=(17^h44^m00^s.0, -29°13′40″.9) [$(l, b)=(359^\circ566, +0^\circ149)$], and hence we named this source Suzaku J174400–2913. Comparing with the Chandra image, we found that Suzaku J174400–2913 coincides with the “X-ray thread” G359.55+0.16 (Wang et al. 2002; Lu et al. 2003; Johnson et al. 2009).

3.2. Spectrum

X-ray spectra of Suzaku J174400–2913 were extracted from an ellipse with the major and minor radii of 2′ and 1′, respectively. Taking account of the large b -dependence of the GCXE flux (e.g., Yamauchi et al. 1990; Uchiyama et al. 2013), we extracted the background spectra from a nearby source-free region with the same b as the source. The source and the background regions are shown by the solid and dotted lines, respectively in figure 1.

We constructed the non-X-ray background (NXB) for the source and the background spectra from the night-earth data (version 2013-06-01) using `xisnxbgen` (Tawa et al. 2008). For both the NXB-subtracted source and background spectra, we made vignetting correction according to the method shown by Hyodo et al. (2008), and subtracted the background spectra from the source spectra. The source count rates after the background subtraction were $(4.5\pm0.7)\times10^{-3}$, $(4.5\pm0.7)\times10^{-3}$, and $(5.2\pm0.7)\times10^{-3}$ counts s^{-1} in the 2–8 keV band for XIS 0, XIS 1, and XIS 3, respectively. Then we merged the XIS 0 and XIS 3 spectra, because the response functions of the FIs are essentially the same with each other. The background-subtracted source spectra are shown in figure 2. In the spectra, we see strong emission lines at ~ 6.7 keV.

Since Chandra resolved many point sources in the background and source regions (e.g., Munro et al. 2004; Munro et al. 2009), we examined the contribution of the point sources. The source region of Suzaku J174400–2913 contains 11 Chandra sources. The integrated photon flux of the point sources is $(1.41\pm0.21)\times10^{-5}$ photons s^{-1} cm^{-2} in the 2–8 keV energy band (the Chandra GC source catalog, Munro et al. 2009). The background region contains 21 sources, then the integrated photon flux is $(2.25\pm0.22)\times10^{-5}$ photons s^{-1} cm^{-2} in the 2–8 keV band. Since the area of the background region is about 3 times larger than the source region, 7.0×10^{-6} photons s^{-1} cm^{-2} (2–8 keV) should be remained in the source spectra, if a simple background subtraction is made (only difference of area is corrected). Thus we must estimate the remaining point source spectra for the spectral fitting by making a model spectrum of the Chandra point sources.

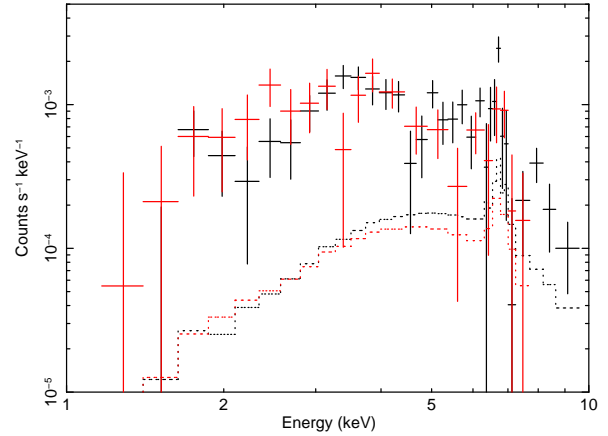


Fig. 2. X-ray spectra of Suzaku J174400–2913 (black: XIS 0+3 and red: XIS 1). The dotted lines show the contribution of the residual Chandra point sources.

Since the photon numbers of the Chandra sources in the source region are limited to make a model spectra, less than 80 counts each, we made a model spectrum using the integrated data of all the Chandra point sources with smaller than 80 net counts (Table 4 in Munro et al. 2004). The normalization was adjusted to become the photon flux to be 7.0×10^{-6} photons s^{-1} cm^{-2} (2–8 keV). The contribution of the remaining point sources to the source count rate in the 2–8 keV band was estimated to be 14–19 %. The estimated spectrum of the remaining point sources is plotted in figure 2. Still we clearly see excess emission above the point source model.

We used the response files, Redistribution Matrix Files (RMFs) and Ancillary Response Files (ARFs) taken from `xismfgen` and `xissimarfgen`, respectively. For the excess emission, we simultaneously fitted the XIS 0+3 and the XIS 1 spectra with an absorbed power-law function. The cross sections of photoelectric absorption were taken from Morrison and McCammon (1983). This model was rejected with a 90% confidence level (a χ^2 value of 72.4 for d.o.f.=52), remaining large excess at ~ 6.7 keV. Thus we added a narrow Gaussian line at $6.71(\pm0.05)$ keV, then the fit was significantly improved with the $\Delta\chi^2$ value of 13.4, which is statistically highly significant of more than 99 % confidence level. The equivalent width was 850^{+400}_{-390} eV. Thus, we conclude that Suzaku J174400–2913 has a prominent 6.7 keV emission line, indicating a thin thermal origin.

Then we applied a thin thermal plasma model in a collisional ionization equilibrium state (`appec` model in XSPEC) modified by low energy absorption. The abundances were taken from Anders and Grevesse (1989). This model also gave an acceptable fit with $\chi^2/d.o.f.=59.2/51=1.16$. The best-fit model is plotted in figure 3.

Since the remaining point source photon flux has an error of 31% (90% confidence level), we examined the best-fit parameters and their errors by changing the intensity (normalization) of the remaining point source spectrum

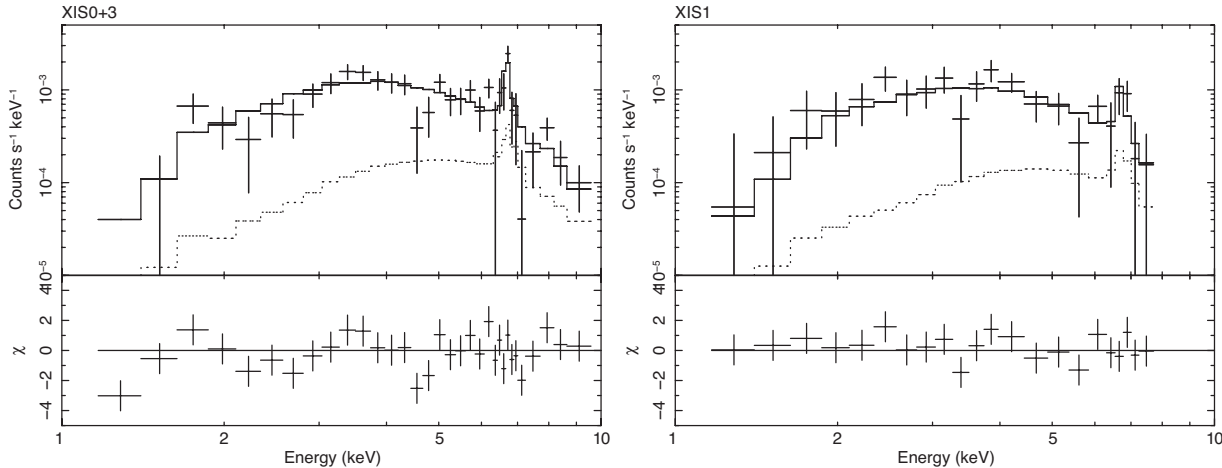


Fig. 3. X-ray spectra of Suzaku J174400–2913 (upper panel) and the residuals from the best-fit model (lower panel), left: XIS 0+3 and right: XIS 1. The solid lines show the best-fit model, while the dotted lines show the contribution of the residual point source model.

Table 1. Spectral parameters of Suzaku J174400–2913.

Parameter	Value
Diffuse: $wabs \times apec$	
N_H ($\times 10^{22}$ cm^{-2})	$6.1^{+2.5}_{-1.3}$
kT (keV)	$4.1^{+2.7}_{-1.8}$
Abundance* (Solar)	$0.58^{+0.41}_{-0.32}$
Normalization [†]	$5.4^{+5.1}_{-1.9} \times 10^{-4}$
$\chi^2/d.o.f.$	59.2/51

* Relative to the solar value (Anders & Grevesse 1989).

[†] The unit is $10^{-14} \times VEM / (4\pi d^2)$, where VEM is the volume emission measure [cm^{-3}] and d is the distance [cm].

by $\pm 31\%$. The results are listed in table 1. The N_H value and the flux of Suzaku J174400–2913 in the 2–8 keV band are $6.1^{+2.5}_{-1.3} \times 10^{22}$ cm^{-2} and 2.5×10^{-13} $erg\ s^{-1}\ cm^{-2}$, respectively.

3.3. Time Variability

In order to examine time variability, we made light curves in the 2–8 keV band from the source region for each detector. After the background subtraction, the data of XIS 0, 1, and 3 were merged. After the timing data were grouped for a 512 s bin, the light curve was fitted with a constant flux model. The $\chi^2/d.o.f.$ value was 276/321=0.86, and hence no significant intensity variation was found.

4. Discussion

The best-fit N_H value of 6.1×10^{22} cm^{-2} is consistent with that of the GC (e.g., Sakano et al. 2002), and hence we assume that Suzaku J174400–2913 is located near the GC, a 8 kpc distance from the Sun in the following discussion.

Suzaku J174400–2913 was stable in the short time scale during the Suzaku observation. The observed energy flux of Suzaku J174400–2913 is roughly consistent with that of the X-ray thread G359.55+0.16 (Johnson et al. 2009). Thus we see no noticeable time variability in the short and long time scale. Furthermore, a power-law model fit for the XIS spectra gave a photon index of $2.3^{+1.0}_{-0.8}$ and an N_H value of $6.5^{+3.3}_{-2.1} \times 10^{22}$ cm^{-2} , which are consistent with those from Chandra within the errors (Johnson et al. 2009). These facts support that Suzaku J174400–2913 is a diffuse source and is associated with G359.55+0.16. Contrary to Lu et al. (2003) and Johnson et al. (2009), we concluded that Suzaku J174400–2913=G359.55+0.16 is thermal origin. The Chandra spectrum had a lower signal-to-noise ratio and the data below 6.7 keV were used for the spectral analysis (Lu et al. 2003; Johnson et al. 2009), which would be the reason that Chandra could not detect the 6.7 keV line.

Since the Suzaku point spread function is not good enough to determine the spatial structure, we assume the geometry of Suzaku J174400–2913 to be a cylinder with a diameter of $10''$ and a length of $2'$ (Lu et al. 2003). Then the volume, V , was estimated to be 1.6×10^{55} cm^3 . Using the best-fit volume emission measure of Suzaku J174400–2913, 4.1×10^{56} cm^{-3} , and $n_e = 1.2n_H$, where n_e and n_H are the electron and hydrogen densities, respectively, we calculated the mean hydrogen and electron densities to be $n_H = 4.6$ cm^{-3} and $n_e = 5.5$ cm^{-3} , respectively. The total thermal energy, E_{th} , and the gas mass, M , were $E_{th} = (3/2)(n_H + n_e)kTV = 1.6 \times 10^{48}$ erg and $M = 1.4n_H m_H V = 0.09M_\odot$, respectively, where k , T and m_H are the Boltzmann constant, the plasma temperature, and the hydrogen mass, respectively.

Chandra and XMM-Newton discovered many X-ray filamentary structures in the GC (e.g., Wang et al. 2002; Sakano et al. 2003; Lu et al. 2003, 2008; Johnson et al. 2009). Among them, only G359.942–0.03 exhibited an emission line at ~ 6.7 keV (Johnson et al. 2009). It

has a point-like near-infrared source found in the Two-Micron All-Sky Survey (2MASS) (Skrutskie et al. 2006) and a comet-like tail. Johnson et al. (2009) proposed that G359.942–0.03 is a ram pressure confined stellar wind bubble generated by a massive star.

Suzaku J174400–2913 is also filamentary but with no core. Thus it may not be stellar wind bubbles like G359.942–0.03. Since Suzaku J174400–2913 is aligned with the NTF G359.54+0.18 (Yusef-Zadeh et al. 1997; Lu et al. 2003), it may be a part of the GCXE confined by the magnetic field. In fact, recent near infrared observations suggest that the GCXE could be confined by the magnetic field in the GC region (Nishiyama et al. 2013). The thermal pressure, p_{th} , is calculated to be $p_{\text{th}}=(n_{\text{H}}+n_{\text{e}})kT\sim 6.6\times 10^{-8}$ dyn cm $^{-2}$. Assuming that the thermal pressure is equal to the magnetic pressure, we can estimate the magnetic field strength to be 1.3 mGauss.

Related to the origin of the GCXE, we note here the other diffuse thermal sources with a ~ 6.7 keV line in the GC region. Suzaku found an elongated source along the Galactic plane in the Sgr B2 region named G0.61+0.01 (Koyama et al. 2007b). They predicted that G0.61+0.01 is a part of a young SNR. From the filament-like morphology, an alternative scenario would be possible: G0.61+0.01 may also be a confined filament by the magnetic field, although the NTF has not been found near the source. The magnetic field is estimated to be ~ 0.4 – 0.5 mGauss. These magnetic field strengths are comparable to those observed in the GC region, 0.1–1 mGauss (e.g., Anantharamaiah et al. 1991; Morris & Serabyn 1996). Senda et al. (2002) discovered the other thermal source with a strong Fe K-shell line, G0.570–0.018 using Chandra. G0.570–0.018 has a ring-like structure with a radius of $10''$ and a tail-like structure. They predicted to be a very young supernova remnant possibly in a free expansion phase. It was also detected with XMM-Newton and Suzaku (Inui et al. 2009), suggesting that the 6.4 keV line was variable, while the 6.7 keV line was stable. The origin of the variable 6.4 keV line would be due to X-ray reflection nebula (Koyama et al. 1996), while the stable 6.7 keV line and the plasma temperature of 6.1 keV are very similar to those of the GCXE. Thus these thermal sources including Suzaku J174400–2913 would contribute to the GCXE. We suggest further deep survey observations may reveal many thermal sources in the GC region.

Acknowledgement

The authors are grateful to all members of the Suzaku team. This work was supported by the Japan Society for the Promotion of Science (JSPS) KAKENHI Grant Numbers, 24540232 (S. Y.), 24740123 (M. N.), and 24540229 (K. K.).

References

Anantharamaiah, K. R., Pedlar, A., Ekers, R. D., & Goss, W. M. 1991, *MNRAS*, 249, 262
 Anders, E., & Grevesse, N. 1989, *Geochim. Cosmochim. Acta*,

53, 197
 Baganoff, F. K., et al. 2001, *Nature*, 413, 45
 Baganoff, F. K., et al. 2003, *ApJ*, 591, 891
 Eckart, A., Genzel, R., Ott, T., & Schödel, R. 2002, *MNRAS*, 331, 917
 Genzel, R., & Townes, C. H. 1987, *ARA&A*, 25, 377
 Genzel, R., Hollenbach, D., & Townes, C. H. 1994, *Rep. Prog. Phys.*, 57, 417
 Genzel, R., Pichon, C., Eckart, A., Gerhard, O. E., & Ott, T. 2000, *MNRAS*, 317, 348
 Ghez, A. M., Morris, M., Becklin, E. E., Tanner, A., Kremenek, T. 2000, *Nature*, 407, 349
 Hyodo, Y., Tsujimoto, M., Hamaguchi, K., Koyama, K., Kitamoto, S., Maeda, Y., Tsuboi, Y., & Ezoe, Y. 2008, *PASJ*, 60, S85
 Inui, T., Koyama, K., Matsumoto, H., & Tsuru, T. G. 2009, *PASJ*, 61, S241
 Johnson, S. P., Dong, H., & Wang, Q. D. 2009, *MNRAS*, 399, 1429
 Koyama, K., Awaki, H., Kunieda, H., Takano, S., Tawara, Y., Yamauchi, S., Hatsukade, I., & Nagase, F. *Nature*, 1989, 339, 603
 Koyama, K., Maeda, Y., Sonobe, T., Takeshima, T., Tanaka, Y., & Yamauchi, S. *PASJ*, 1996, 48, 249
 Koyama, K., et al. 2007a, *PASJ*, 59, S23
 Koyama, K., et al. 2007b, *PASJ*, 59, S221
 Koyama, K., et al. 2007c, *PASJ*, 59, S245
 Lu, F. J., Wang, Q. D., & Lang, C. C. 2003, *AJ*, 126, 319
 Lu, F. J., Yuan, T. T., & Lou, Y. -Q. 2008, *ApJ*, 673, 915
 Mitsuda, K., et al. 2007, *PASJ*, 59, S1
 Morris, M., & Serabyn, E. 1996, *ARA&A*, 34, 645
 Morrison, R., & McCammon, D. 1983, *ApJ*, 270, 119
 Muno, M. P., et al. 2004, *ApJ*, 613, 1179
 Muno, M. P., et al. 2009, *ApJS*, 181, 110
 Nakajima, H., et al. 2008, *PASJ*, 60, S1
 Nishiyama, S., et al. 2013, *ApJ*, 769, L28
 Ponti, G., Terrier, R., Goldwurm, A., Belanger, G., & Trap, G. 2010, *ApJ*, 714, 732
 Ryu, S. G., Nobukawa, M., Nakashima, S., Tsuru, T. G., Koyama, K., & Uchiyama, H. 2013, *PASJ*, 65, 33
 Sakano, M., Koyama, K., Murakami, H., Maeda, Y., & Yamauchi, S. 2002, *ApJS*, 138, 19
 Sakano, M., Warwick, R. S., Decourchelle, A., & Predehl, P. 2003, *MNRAS*, 340, 747
 Schödel, R., et al. 2002, *Nature*, 419, 694
 Senda, A., Murakami, H., & Koyama, K. 2002, *ApJ*, 565, 1017
 Serlemitsos, P., et al. 2007, *PASJ*, 59, S9
 Skrutskie, M. F., et al. 2006, *AJ*, 131, 1163
 Tawa, N., et al. 2008, *PASJ*, 60, S11
 Uchiyama, H., et al. 2009, *PASJ*, 61, S9
 Uchiyama, H., Nobukawa, M., Tsuru, T. G., & Koyama, K. 2013, *PASJ*, 65, 19
 Wang, Q. D., Gotthelf, E. V., & Lang, C. C. 2002, *Nature*, 415, 148
 Yamauchi, S., Kawada, M., Koyama, K., Kunieda, H., Tawara, Y., & Hatsukade, I. 1990, *ApJ*, 365, 532
 Yusef-Zadeh, F., Morris, M., & Chance, D., 1984, *Nature*, 310, 557
 Yusef-Zadeh, F., Wardle, M., & Parastaran, P., 1997, *ApJ*, 475, L119